Are penny-shaped cracks a good model for compliant porosity?

Boris Gurevich, Curtin Univ. and CSIRO Petroleum, Dina Makarynska, Curtin Univ., and Marina Pervukhina, CSIRO Petroleum, Perth, Australia

Summary

Variation of elastic properties of rocks with pressure is often modeled using penny-shaped or spheroidal cracks as idealization of real crack/pore geometry. We analyze the validity of this approach by extracting the ratios of shear to bulk stress sensitivity coefficients, and normal to tangential compliances from ultrasonic measurements on 76 dry sandstone samples. Comparison of these ratios against the predictions of the spheroidal crack theory shows that for roughly half of the samples, the ratio of normal to tangential compliance is significantly lower than predicted by spherodical crack theory. This inconsistency results in significantly different estimates of crack density from bulk and shear moduli, and in deviation of predicted pressure variation of Poisson's ratio from the measured data.

Introduction

Understanding and modeling of the effect of pressure and stress on elastic properties of rocks is important for such diverse applications as lithology and fluid identification in presence of mechanical compaction, pore pressure prediction, and analysis of time-lapse response to fluid injection and depletion. Laboratory measurements on porous rocks show that increase of pressure from zero to typical reservoir pressures causes substantial (up to 50%) increase of bulk and shear moduli, but only small (below 1%) reduction in overall porosity. This suggests that pressure dependency of elastic properties is caused by preferential closure of very compliant pores with small overall volume but large specific surface area. Perhaps the simplest shape that captures such properties is a so-called penny-shaped crack: an oblate spheroid (ellipsoid of revolution) whose aspect ratio (ratio of smaller to larger semi-axis) is a small parameter (say, from 10^{-4} to 10^{-2}). In granular rocks these compliant pores (cracks) most likely occur at grain contacts or as intra-granular micro-fractures.

Pores are modeled by ellipsoids not because anyone believes pore space consists of ellipsoids, but because they (1) appear to capture some essential properties of subsurface voids, (2) provide intuitively simple parameterization of enormous complexity of the real pore space, and (3) are relatively easily amenable to theoretical analysis. For a given porosity, the smaller is the (mean) aspect ratio of the pores, the stronger is the effect of these pores on the overall rock stiffness. For this reason, aspect ratios or their distributions are often used as lithology indicators. However, aspect ratio is also a function of (effective) pressure, as pores of small aspect ratio are more compliant and thus close preferentially under pressure – one more reason to study compliant pores in more detail.

The model of spheroidal pores is intuitively appealing (with obvious reservations), but is it quantitatively adequate? As mentioned above, complaint pores cause a reduction in bulk and shear moduli. This reduction occurs because each crack adds a little extra compliance to the rock – reducing both resistance to compression in the direction normal to its surface (normal compliance) and resistance to shear in the same plane (shear or tangential compliance). Since we can only measure the overall effect of these cracks, we cannot compute the normal or shear compliances for an individual crack, but we can compute the ratio of normal to shear compliances from measurements. Expressions for both normal and tangential compliances caused by an ellipsoidal crack are well known, and their ratio can be easily computed. In this paper, we will assess the adequacy of the penny-shaped crack model by comparing the compliance ratio obtained from measurements against the theoretical expression for penny-shaped cracks.

Method

Our first objective is to obtain the ratio of normal to tangential compliance from ultrasonic measurements. For simplicity, we will only consider isotropic rocks. Similar analysis for anisotropic rocks is also possible if full elastic tensor measurements are available (Verdon et al., 2008). For isotropic materials, Sayers and Han (2002) proposed an elegant approach to computing normal to shear compliance ratio from measured bulk and shear moduli. They assumed that a rock at the highest available confining pressure has no compliant porosity, and that reduction of the moduli at lower pressures occurs due to the presence of isotropically distributed compliant cracks. For the isotropic case, the general additive compliance equations of Sayers and Kachanov (1995) give the following expressions for dry bulk and shear moduli

$$\frac{1}{K}=\frac{1}{K_h}+sB_N, \tag{1}$$

$$\frac{1}{\mu}=\frac{1}{\mu_h}+\frac{4}{15}sB_N+\frac{2}{5}sB_T, \tag{2}$$

where K and μ are the dry bulk and shear moduli of the rock at a given confining pressure P, K_h and μ_h are the bulk and shear moduli of a hypothetical rock without the compliant porosity ("Swiss cheese"), B_N and

B_T are the normal and shear compliances of an individual crack, and s is the total area of the cracks. If for a given sample, moduli K_h and μ_h at the highest pressure P_h and moduli K and μ at a given pressure $P < P_h$ are measured, equations (1) and (2) can be easily solved for sB_N and sB_T. Sayers and Han (2002) used this approach to obtain the ratio $B = B_N / B_T$ from dry and saturated sandstone ultrasonic velocities measured by Han et al. (1986). Their results show that for dry rocks, most values of *B* lie between 0.25 and 1.5, with a few values between 1.5 and 3. Similar results for dry anisotropic rocks were obtained by Verdon et al. (2008).

According to Sayers and Kachanov (1995) the ratio *B* for dry penny-shaped cracks is

$$B = 1 - \nu/2\,, \tag{3}$$

where ν is Poisson's ratio. The results of Sayers and Han (2002) appear to be inconsistent with the penny-shape prediction. However there is still uncertainty about the validity about experimental *B* values due to the following factors

- Some of the samples studied by Han (1986) show the moduli still increasing with pressure even when they approach the highest pressure (50 MPa). This suggests that either not all compliant pores are closed at the highest pressure, or reduction of stiff porosity contributes to the increase of the moduli.
- The propagation of measurement errors causes large relative errors of B values in the upper part of the pressure range, where both normal and shear compliances are small.

In an attempt to attain compliance ratios with higher degree of confidence, we use the theory of Shapiro (2003), who recently proposed an alternative approach to modeling stress sensitivity. Shapiro showed that well known exponential dependency of elastic moduli on pressure can be written in the form

$$\frac{1}{K} = \frac{1}{K_h} + \frac{\theta_s P}{K_h} + \frac{1}{K_h}\theta_c\phi_c, \tag{4}$$

and

$$\frac{1}{\mu} = \frac{1}{\mu_h} + \frac{\theta_{s\mu} P}{\mu_h} + \frac{1}{\mu_h}\theta_\mu\phi_c, \tag{5}$$

where θ_c and θ_μ are bulk and shear stress sensitivity parameters due to compliant porosity, θ_s and $\theta_{s\mu}$ are corresponding parameters due to (weak) compression of stiff porosity, and $\phi_c(P)$ is compliant porosity given by

$$\phi_c = \phi_{c0}\exp\left(-\theta_c P / K_h\right). \tag{6}$$

The consistency of Shapiro's (2003) theory with experiment was recently demonstrated by Pervukhina et al. (2009) who compared the values of compliant porosity obtained from fitting equations (4) and (5) to data against direct porosity data obtained from measured strain.

Comparing Shapiro's equations (4) and (5) with equations (1) and (2), we can see that they are mutually consistent. In essence, ignoring the stiff porosity effect for a moment, we can view Shapiro's equations as a particular variant of Sayers-Kachanov (1995) equations with normal and tangential compliances defined as

$$sB_N = \frac{\theta_c}{K_h}\phi_{c0}\exp\left(-\theta_c P / K_h\right) \tag{7}$$

and

$$sB_T = \left(\frac{5}{2}\frac{\theta_\mu}{\mu_h} - \frac{2}{3}\frac{\theta_c}{K_h}\right)\phi_{c0}\exp\left(-\theta_c P / K_h\right), \tag{8}$$

so that

$$B = \frac{B_N}{B_T} = \frac{1}{\dfrac{5K_h\theta_\mu}{2\mu_h\theta_c} - \dfrac{2}{3}} \tag{9}$$

or

$$B = \frac{B_N}{B_T} = \frac{3}{\dfrac{5(1+\nu_h)\theta_\mu}{(1-2\nu_h)\theta_c} - 2}\,, \tag{10}$$

where ν_h is Poisson's ratio of the rock in high-pressure limit, where all compliant porosity is closed. Note that ϕ_c / s is some effective thickness of compliant pores. Shapiro (2003) showed that linear terms in equations (4) and (5) are often small compared with the exponential terms. Thus the compliance ratio can be obtained by fitting equations (4) and (5) to measured elastic moduli functions of pressure, computing the ratio of stress sensitivity parameters $q = \theta_\mu / \theta_c$, and then computing compliance ratio *B* using equation (10). Note that in the theory of Shapiro (2003), the compliance ratio *B* is independent of pressure. The consistency of this conclusion with experimental data was analyzed by Pervukhina et al. (2009) and Verdon et al. (2008).

Application to sandstone data

Stress sensitivity coefficients and corresponding values of compliance ratio have been computed for ultrasonic measurements on 76 dry sandstone samples as reported in Han et al. (1986) and in Grochau and Gurevich (2008). Figure 1 shows *q* ratios computed for all samples as a function of Poisson's ratio ν_h in the limit of large pressure (blue squares). The line passing through each circle shows confidence limits for *q* ratio and Poisson's ratio as discussed below. Red solid line shows the dependency of

$q(\nu_h)$ as predicted by Shapiro and Kaselow (2005) for the special case of an isotropic rock with porosity tensor of special symmetry. Red dashed line shows the ratio of stress sensitivities as predicted by non-interactive approximation for spheroidal cracks. From the first glance at Figure 1 we can see that

- Compliance ratios predicted by Shapiro and Kaselow is almost identical to that for spheroidal cracks
- Ultrasonic data on stress sensitivity ratio show large scatter and do not show much correlation with Poisson's ratio.

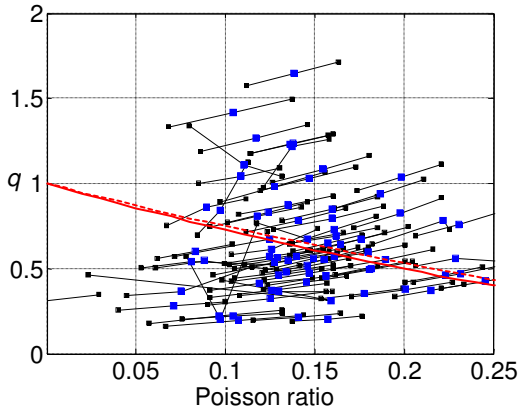

Figure 1: Stress sensitivity ratio q estimated from ultrasonic velocity measurements on 76 dry samples (blue squares), errobars due to systematic errors in shear velocities (black lines and squares), scalar cracks (solid red line), and spheroidal cracks (dashed red line).

As mentioned earlier, the aim of this paper is to analyze what values of stress sensitivity ratio and compliance ratio are realistic. To this end, we performed extensive error and sensitivity analysis. Influence of the following factors has been analyzed.

Effect of the linear (stiff porosity) term in equations (4) - (5) was analyzed by comparing quality of the fit to data with and without these terms. To our surprise, in all but 5% of samples, inclusion of the linear term reduces the misfit to much larger extent than expected due to the increase of the number of degrees of freedom. Thus we conclude that the deformation of stiff porosity plays significant role in defining stress dependency of elastic properties of rocks.

We also analyzed the sensitivity of the results to systematic errors in velocity picking. This was done by assuming that all shear wave velocities were misestimated by ±50 m/s, and re-computing all the results. These results are shown in Figure 1 as the end points of the error bars. As expected, the relative error introduced is much larger for Poisson ratios than for stress sensitivity ratios.

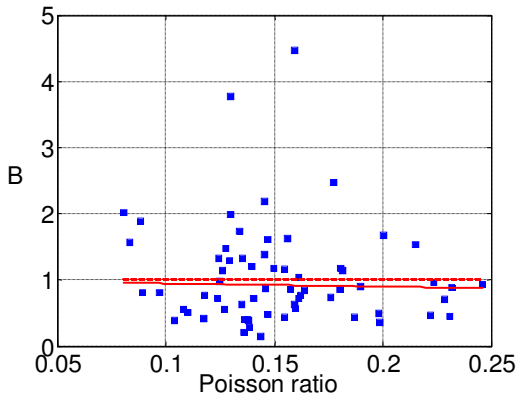

Figure 2: Compliance ratio B from ultrasonic velocity measurements on 64 dry samples with systematic errors less than 100% (blue squares), theory for scalar cracks (solid red line), and spheridal cracks (dashed red line)

We also analyzed the effect of random errors, computed using standard error propagation analysis and χ^2 criterion.

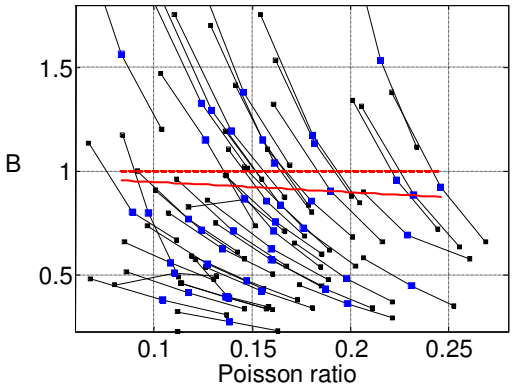

Figure 3: Compliance ratio B estimated from ultrasonic velocity measurements on 49 dry samples (blue squares) with systematic errors less than 40% (black lines and squares), scalar cracks (solid red line), and spheroidal cracks (dashed red line).

Random errors create a thin confidence tube-shaped area around the systematic error bar. For all but a handful of really bad samples, the influence of these random errors turns out to be negligibly small compared to model errors and systematic errors discussed above.

The stress sensitivity estimates shown in Figure 1 were used to compute compliance ratios using equation (10). The resulting estimates of B ratio are shown in Figure 2. Since B ratios show much larger scatter than q ratios, in Figure 2 we only show the results for samples where the relative

Penny-shaped cracks as a model for soft pores

error in B caused by systematic shear velocity errors is less than 100% per cent (64 out of 76 samples; error bars are not shown to avoid clutter). The solid red line $B=1$ corresponds to stress-sensitivity ratio as suggested by Shapiro and Kaselow (2005), and earlier by Sayers and Kachanov (1991) (so-called scalar cracks). The solid line corresponds to non-interaction approximation for spheroidal cracks. We see that the B ratios are mostly scattered between 0 and 2, with no visible correlation with Poisson's ratios.

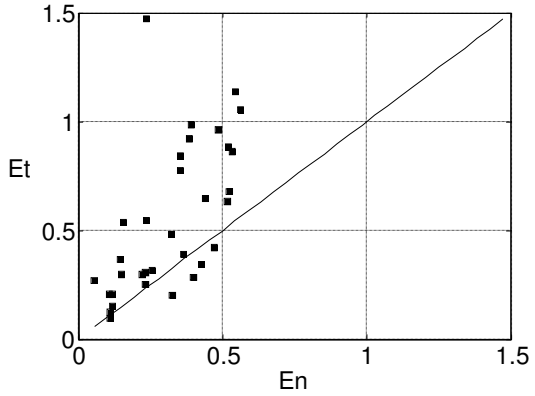

Figure 4: Crack density (Et) extracted from shear modulus against crack density (En) extracted from bulk modulus.

In Figure 3 we show the error bars for those samples with systematic (relative) errors in B ratio below 50% (49 samples). We see that

- Errors in B (vertical spread of the error bar) are much larger than for q ratio. This is understandable, as errors in Poisson's ratio propagate into B when the latter is computed using equation (10).
- For most samples the vertical spread of the error bar far exceeds the difference between B values for spheroidal cracks, equation (3), and for 'scalar' cracks ($B=1$).
- Where $B>1$, one or both ends of the error bar appears to cross or approach the line $B=1$.

To check this last observation, we select only those samples for which the error bar corresponding to systematic shear velocity errors does not enter the band $0.9<B<1.1$. This leaves 19 samples (40% out of those with errors below 50%). Importantly, all but one of these selected samples have values $B<1$. This allows us to make an important conclusion: where B can be confidently said to be significantly different from 1, it is always smaller than 1.

What is the effect of compliance ratio B being smaller than predicted by spheroidal crack theory? One effect is that if we estimate crack density from bulk or shear modulus, the results will be different. These estimates are plotted in Figure 4 against one another for those samples with relative errors below 50%. We see that for roughly half of these samples, the crack density predicted from shear compliance is significantly higher than that from the bulk modulus. This graphically illustrates that the measured data on sandstones is inconsistent with spheroidal crack theory.

To show the meaning of various B values, in Figure 5 (a-c) we show stress dependency of Poisson's ratio obtained from measurements (symbols) against that predicted by spheroidal crack theory. We see that when compliance ratio is significantly different from 1, the prediction of the spherodial crack theory deviates from measured data.

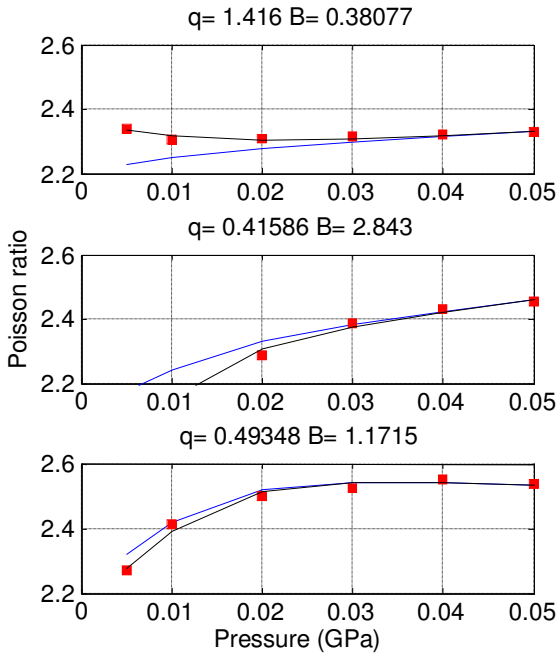

Figure 5: Pressure variation of Poisson's ratio for a number of samples computed from measured velocities (symbols), predicted by Sayers-Kachanov (1995) and Shapiro (2003) theory (black line) and by spherodical crack theory (blue line).

Conclusions

The ratio of shear to bulk stress sensitivities shows large scatter and, for a large number of dry sandstone samples, is not consistent with either the "scalar" crack approximation or spherodial crack theory.

The ratio of normal to tangential compliance shows large scatter, with most values between 0 and 2. Values over 1 have higher relative errors. Data with relative systematic errors below 50% show compliance ratios close to or below 1. About half of those are inconsistent with the spheroidal crack theory.

EDITED REFERENCES

Note: This reference list is a copy-edited version of the reference list submitted by the author. Reference lists for the 2009 SEG Technical Program Expanded Abstracts have been copy edited so that references provided with the online metadata for each paper will achieve a high degree of linking to cited sources that appear on the Web.

REFERENCES

Grochau, M. H., and B. Gurevich, 2008, Investigation of core data reliability to support time-lapse interpretation in Campos Basin, Brazil: Geophysics, **73**, no. 2, E59–E65.

Han, D.-H., 1986, Effects of porosity and clay content on acoustic properties of sandstones and unconsolidated sediments: Ph.D. thesis, Stanford University.

Han, D.-H., A. Nur, and D. Morgan,1986, Effects of porosity and clay content on wave velocities in sandstones: Geophysics, **51**, 2093–2107.

Pervukhina, M., B. Gurevich, D. N. Dewhurst, and A. F. Siggins, 2009, Experimental verification of the physical nature of velocity-stress relationship for isotropic porous rocks: Geophysical Journal International, (submitted for publication).

Sayers C. M., and D.-H. Han, 2002, The effect of pore fluid on the stress-dependent elastic wave velocities in sandstones: 72nd Annual International Meeting, SEG, Expanded Abstracts, 1842–1845.

Sayers, C. M., and M. Kachanov, 1991, A simple technique for finding effective elastic constants of cracked solids for arbitrary crack orientation statistics: International Journal of Solids and Structures, **12**, 81–97.

Sayers, C. M., and M. Kachanov, 1995, Microcrack induced elastic wave anisotropy of brittle rocks: Journal of Geophysical Research, **100**, 4149–4156.

Shapiro, S. A., 2003, Elastic piezosensitivity of porous and fractured rocks: Geophysics, **68**, no. 2, 482–486.

Shapiro, S. A., and A. Kaselow, 2005, Porosity and elastic anisotropy of rocks under tectonic stress and pore-pressure changes: Geophysics, **70**, no. 5, N27–N38.

Verdon, J. P., D. A. Angus, J. M. Kendall, and S. A. Hall, 2008, The effect of microstructure and nonlinear stress on anisotropic seismic velocities: Geophysics, **73**, no. 4, D41–D51.